JOURNAL OF VIROLOGY, May 2004, p. 5368–5381 Vol. 78, No. 10
0022-538X/04/$08.00+0 DOI: 10.1128/JVI.78.10.5368–5381.2004

Analysis of Adenovirus Sequestration in the Liver, Transduction of Hepatic Cells, and Innate Toxicity after Injection of Fiber-Modified Vectors

Dmitry M. Shayakhmetov,[1] Zong-Yi Li,[1] Shaoheng Ni,[1] and André Lieber[1,2]*

Division of Medical Genetics[1] and Department of Pathology,[2] University of Washington, Seattle, Washington 98195

Received 20 November 2003/Accepted 12 January 2004

After intravenous administration, adenovirus (Ad) vectors are predominantly sequestered by the liver. Delineating the mechanisms for Ad accumulation in the liver is crucial for a better understanding of Ad clearance and Ad-associated innate toxicity. To help address these issues, in this study, we used Ad vectors with different fiber shaft lengths and either coxsackievirus-Ad receptor (CAR)-interacting Ad serotype 9 (Ad9) or non-CAR-interacting Ad35 fiber knob domains. We analyzed the kinetics of Ad vector accumulation in the liver, uptake into hepatocytes and Kupffer cells, and induction of cytokine expression and release in response to systemic vector application. Immediately after intravenous injection, all Ad vectors accumulated equally efficiently in the liver; however, only genomes of long-shafted Ads were maintained in the liver tissue over time. We found that Kupffer cell uptake of long-shafted Ads was mediated by the fiber knob domain and was CAR independent. The short-shafted Ads were unable to efficiently interact with hepatocellular receptors and were not taken up by Kupffer cells. Moreover, our studies indicated that Kupffer cells were not the major reservoir for the observed accumulation of Ads (used in this study) in the liver within the first 30 min after virus infusion. The lower level of liver cell transduction by short-shafted Ads correlated with a significantly reduced inflammatory anti-Ad response as well as liver damage induced by the systemic administration of these vectors. This study contributes to a better understanding of the biology of systemically applied Ad and will help in designing safer vectors that can efficiently transduce target tissues.

Most of the studies on the interactions of adenovirus (Ad) vectors with the host upon systemic application have been done with human Ad serotype 5 (Ad5). Following systemic administration, the clearance of Ad5 from the bloodstream and its accumulation in the liver occur within minutes (2, 4, 21). This phenomenon is thought to be due to the tissue architecture and vascular systems of the liver. Intravenously injected Ad particles reach the liver through the portal vein and contact most hepatocytes only after passing through the liver sinusoids, the walls of which are formed by endothelial cells. Sinusoid endothelial cells have fenestrae of ~100 nm. These fenestrae of the sinusoidal lumen allow communication with the space of Disse, which is in direct contact with hepatocytes because of the lack of a continuous basement membrane. Kupffer cells are located on the inside of the sinusoidal wall. The fenestration within the sinusoidal wall allows Ad5 particles (which have an average diameter of 80 nm) to efficiently translocate from the plasma to hepatocytes. Both hepatocytes and Kupffer cells efficiently take up Ad5 particles (2, 19, 21, 34, 51, 52).

In vitro, Ad5 vectors use a two-step mechanism to infect cells. The first step is a high-affinity interaction between the Ad fiber knob and the coxsackievirus-Ad receptor (CAR) (31), which requires a flexible, long (22-β-repeat) fiber shaft (38, 42, 47, 53). Attachment to CAR is followed by binding of viral penton RGD motifs to cellular integrins, triggering virus internalization (50). However, in vivo, the interaction of Ad5 with CAR and integrins is unlikely to be the major pathway for Ad infection of liver cells. Several studies have documented that mutations that abolish CAR and integrin interactions are not sufficient to eliminate liver transduction (1, 16, 23, 41, 42). Recently, a study by Smith et al. showed that a KKTK motif in the Ad5 fiber shaft binds hepatic heparan sulfate proteoglycans (HSPGs), resulting in liver transduction (42). Furthermore, blood factors appear to bind to the fiber knob domain and mediate uptake through HSPGs (39).

Interestingly, Ad vectors containing short fiber shafts (lacking the KKTK motif) derived from Ad35 (36, 41) or Ad40 (28) (which possess shafts formed by six or seven β repeats) do not efficiently transduce liver cells; these data indicate that for liver uptake, both the blood factor-mediated pathway and the KKTK motif pathway do not function for short-shafted Ads. Vectors containing both the shaft and the knob of Ad35 have become increasingly popular as gene transfer vectors (9, 25, 30, 32, 36, 40, 48) because they are able to transduce a number of important target tissues that are relatively refractory to Ad5 infection, including human hematopoietic stem cells, dendritic cells, and malignant tumor cells. CD46 was recently identified as a cellular receptor for group B Ads, including Ad35 (8, 35). In mice, the expression of CD46 is restricted to the testes (12); this fact explains why mouse cells, including hepatocytes, cannot be infected with Ad35 fiber-containing vectors in vitro (30, 36, 48).

Intravenous Ad injection is associated with the production and release of cytokines (such as interleukin 6 [IL-6], IL-10, IL-8, tumor necrosis factor alpha [TNF-α], and gamma interferon [IFN-γ]) and chemokines (such as MIP-1α and MIP-2) (18, 19, 27) within hours after the intravenous injection of Ad5

* Corresponding author. Mailing address: Division of Medical Genetics, University of Washington, Box 357720, Seattle, WA 98195. Phone: (206) 221-3973. Fax: (206) 685-867. E-mail: lieber00@u.washington.edu.

vectors. These cytokines, in turn, play a major causative role in the pathologic changes (vascular leakage, liver damage, and so forth) associated with intravenous Ad infusion and a role in the induction of an antiviral immune response. Cytokine production and release are thought to be the direct or indirect results of Ad uptake by Kupffer cells and their subsequent activation (18, 19, 27) or lysis (34). Depletion of Kupffer cells by the administration of gadolinium chloride or the intravenous injection of liposomes encapsulating chlodronate (34) followed by the injection of a low dose of Ad (less than 10^9 PFU per mouse) resulted in decreased serum cytokine levels and increased hepatocyte transduction (15, 43, 51). The injection of higher vector doses in combination with Kupffer cell depletion caused increased cytokine levels, liver damage, and decreased transgene expression in hepatocytes (15, 19). These findings indicate that a certain threshold dose of injected Ad can saturate the Kupffer cell capacity for Ad uptake, resulting in the systemic dissemination of Ad particles that can potentially infect other cell types that secrete proinflammatory cytokines; such cell types include nonhepatic (e.g., spleen and lung) macrophages and hepatic endothelial cells (20), peripheral or infiltrating mononuclear cells (11), or stellate cells (5). To this end, studies by Liu et al. (20) have demonstrated that in the absence of Kupffer cells, liver sinusoid endothelial cells are the next cell type to interact directly with Ad vectors through penton RGD motifs.

Understanding the mechanism of and identifying the cell types responsible for Ad clearance and innate toxicity are crucial for the construction of new vectors that are safer and can more efficiently transduce target tissues. In this study, we injected fiber-chimeric Ad vectors intravenously into mice and analyzed the kinetics of Ad vector accumulation in the liver, the efficiency of gene transfer into hepatocytes, the association of the vectors with Kupffer cells, and the expression and release of cytokines that are involved in the induction of an innate immune response.

MATERIALS AND METHODS

Ad vectors. The following Ad vectors, previously constructed and described in detail and expressing green fluorescent protein (GFP) or β-galactosidase reporter genes, were used: Ad5/9L, Ad5/9S, Ad5/35L, and Ad5/35S (38). Ad5/9L and Ad5/9S possess the Ad9 fiber knob domain and the long Ad5 fiber shaft (Ad5/9L) or the short Ad9 fiber shaft (Ad5/9S). Ad5/35L and Ad5/35S possess the Ad35 fiber knob domain and the long Ad5 fiber shaft (Ad5/35L) or the short Ad35 fiber shaft (Ad5/35S).

For comparative analyses, identical GFP (for Ad5/9 vectors) and β-galactosidase (for Ad5/35 vectors) reporter gene expression cassettes were introduced into the E3 region of the Ad genome by homologous recombination in *Escherichia coli* strain BJ5183 as described earlier (40). For amplification, all Ads were used to infect 293 cells under conditions that prevented cross-contamination. Viruses were banded in CsCl gradients, dialyzed, and stored in aliquots as described elsewhere (6). Ad genome titers were determined by quantitative Southern blotting. Virion DNA extracted from purified virus particles for each Ad vector was run on an agarose gel in serial twofold dilutions. As standard DNA of a known concentration (determined spectrophotometrically), we used preparatively purified Ad5 DNA. Standard DNA was applied to the same gel in serial dilutions. After transfer to Hybond N+ nylon membranes (Amersham, Piscataway, N.J.), filters were hybridized with a labeled DNA probe (8-kb HindIII fragment, corresponding to the E2 region of the Ad5 genome), and DNA concentrations were measured with a PhosphorImager (Molecular Dynamics, Sunnyvale, Calif.) for each virus preparation. These values were used to calculate the genome titer for each virus stock used. For each Ad vector used in this study, at least two independently prepared virus stocks were obtained and characterized by determination of PFU titers on 293 cells (24) and determination of genome titers by Southern blotting (40). The genome/PFU ratios were comparable for all vectors used in this study.

Each produced virus stock was tested for endotoxin contamination by using *Limulus* amebocyte lysate Pyrotell (Cape Cod Inc., Falmouth, Mass.). For in vivo experiments, only virus preparations confirmed to be free of endotoxin contamination were used.

Ad infection in vivo. All experimental procedures involving animals were conducted in accordance with the institutional guidelines set forth by the University of Washington. C57BL/6 mice (Charles River, Wilmington, Mass.) were housed in specific-pathogen-free facilities. For analysis of Ad-mediated gene transfer into liver cells, 10^{11} Ad particles (corresponding to 5×10^9 PFU of Ad5/35L vector, determined on 293 cells) in 200 μl of phosphate-buffered saline (PBS) were injected by tail vein infusion. For in vivo transduction studies, mice were sacrificed at 72 h after virus infusion and livers were processed for histological analysis. For analysis of Ad genome accumulation in liver tissue, at 30 min, 6 h, and 24 h after Ad vector administration into the tail vein, the blood was flushed from the liver with a cardiac saline perfusion, the liver was harvested, and total DNA was purified as described earlier (36).

To analyze Ad association with purified hepatocytes, at 30 min after tail vein vector application, mouse livers were perfused for 15 min with a collagenase solution via a catheter permanently placed into the portal vein (49). Then, partially disintegrated livers were carefully removed and dispersed in a collagenase-DNase solution to a single-cell suspension. Following two consecutive washes with 40 ml of PBS containing 2% fetal bovine serum and two differential centrifugations (500 x *g* for 5 min each time), allowing efficient sedimentation of only hepatic parenchymal cells, purified hepatocytes were obtained. Routinely, the purity of hepatic cells obtained by this technique was greater than 90%, according to antialbumin immunochemical staining (data not shown). For further analyses, the purified hepatocytes either were immediately lysed with pronase-sodium dodecyl sulfate buffer for obtaining total cellular DNA or were plated on six-well Primaria plates and cultured for 24 to 48 h. To analyze virus degradation in purified hepatocytes over time, hepatocytes were purified by collagenase perfusion only (see Fig. 4C). At 24 h after plating, hepatocytes were treated with a collagenase-DNase or trypsin-DNase solution for 15 min at 37°C to remove all extracellular virus, washed with PBS, and lysed with pronase-sodium dodecyl sulfate buffer to obtain cellular DNA for subsequent Southern blot analysis. To analyze the efficiency of Ad vector interactions with hepatic cells, livers were perfused for 15 min with 0.25% trypsin–DNase solution prior to collagenase perfusion, and hepatocytes were isolated as described above.

For analysis of reporter gene expression in hepatocytes, at 48 h after purification and plating, photographs of cells were taken under visible light and UV light (for analysis of GFP expression) or cells were fixed and stained in situ for β-galactosidase activity as described earlier (38).

Analysis of Ad-Kupffer cell interactions in vivo. To analyze Ad interactions with Kupffer cells, the Ad vectors were labeled with the fluorophore Cy-3 (37). The titers of Cy-3-labeled vectors were confirmed by quantitative Southern blotting. A total of 10^{11} particles of fluorophore-labeled Ads were injected into the tail vein; 30 min later, livers were flushed with saline via cardiac perfusion, harvested, and immediately frozen in OCT compound (Sakura Finetec Inc., Torrance, Calif.). Frozen liver sections either remained unstained or were stained with rat anti-mouse F4/80 or CD45 primary antibody (BD Biosciences, Palo Alto, Calif.) to detect Kupffer cells. Specific binding of primary antibodies was visualized with secondary anti-rat Alexa Fluor 488 antibody (green) (Molecular Probes, Inc., Eugene, Oreg.). Cy-3-labeled Ad particles appear red. When gadolinium chloride ($GdCl_3$) was used to deplete mice of Kupffer cells, two doses of the drug were injected into mice at 30 h and 6 h before Ad administration as described earlier (19).

Southern blot analysis. Isolation of cellular DNA from mouse livers and Southern analysis were performed as described elsewhere (19). A ^{32}P-labeled 8-kb HindIII fragment, corresponding to the E2 region of the Ad genome, was used for hybridization to specifically detect Ad genomic DNA in livers and purified hepatocytes.

Electron microscopy analysis. For electron microscopy analysis of virus distribution in liver tissue, 10^{11} Ad particles in a total volume of 200 μl of PBS were injected into the tail vein. At 30 min after virus application, livers were harvested, fixed with 2% glutaraldehyde in PBS, and subsequently fixed in 1% OsO_4–phosphate buffer. Then, liver samples were embedded in Medcast (Ted Pella, Redding, Calif.), and ultrathin sections were stained with uranyl acetate and lead citrate. Processed grids were evaluated with a Philips 410 electron microscope operated at 80 kV (magnification, ×21,000). At least two mice were injected with each Ad vector, and the intracellular distribution was analyzed by using multiple liver sections.

Analysis of levels of cytokines, chemokines, and aminotransferases in plasma.

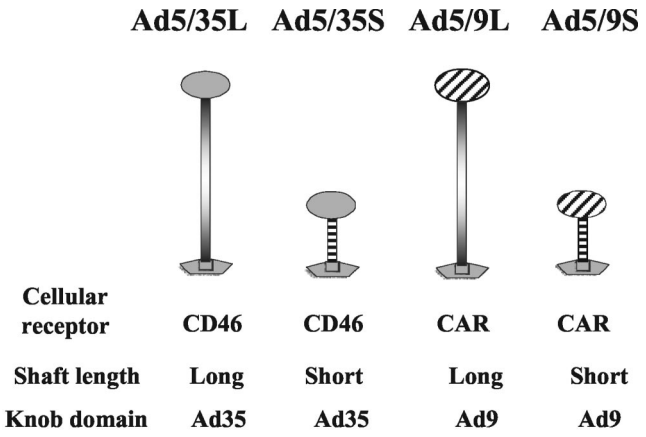

FIG. 1. Schematic representation of Ad fibers and nomenclature of vectors used in this study.

To analyze the levels of proinflammatory cytokines and chemokines in serum, at 30 min, 6 h, and 24 h after intravenous administration of Ad vectors, blood samples were collected in heparin-treated Eppendorf tubes, cells were pelleted for 5 min at 1,000 x *g*, and plasma was obtained and stored at −80°C in small aliquots. To analyze the levels of cytokines and chemokines in plasma, a mouse inflammatory cytometric bead array (BD Biosciences) was used. Briefly, 10 μl of mouse plasma was diluted five times and mixed with cytometric beads capable of binding mouse TNF-α, IL-6, monocyte chemoattractant protein 1, IFN-γ, IL-12p70, and IL-10. The binding of these proteins was detected with corresponding secondary phycoerythrin-conjugated antibodies and analyzed by flow cytometry along with provided standard proteins. The collected data were processed by using the manufacturer's software. Plasma samples obtained from at least three mice (for each Ad vector) were analyzed in duplicate. To analyze the levels of alanine aminotransferase (ALT), a marker of hepatocellular damage, in plasma, a calorimetric ALT detection protocol and reagents (TECO Diagnostics, Anaheim, Calif.) were used according to the manufacturer's protocol without modifications. ALT levels were measured in triplicate by using plasma samples obtained from at least three mice (per Ad).

RNase protection assay. To analyze the mRNA levels for multiple cytokine and chemokine genes in mouse livers, 10^{11} Ad particles were injected into the tail vein; at 30 min, 6 h, and 24 h after virus injection, livers were harvested, and total RNA was extracted by using an RNAqueous-midi kit (Ambion, Inc., Austin, Tex.). Ten μg of total liver RNA was hybridized with a mixture of ^{32}P-labeled RNA probes. The ^{32}P-labeled RNA probe mixture was prepared by in vitro transcription with an in vitro transcription kit and CK-3 and a custom template set provided by Pharmingen (San Diego, Calif.). The hybridized RNA was treated with RNase by using an RNase protection assay kit (Pharmingen) and precipitated, and the protected fragments were resolved on vertical sequencing (10% acrylamide) gels. Following electrophoresis, the gels were dried and exposed to X-ray film (Kodak-X-Omat) and a PhosphorImager screen. The signals on the screen were analyzed with PhosphorImager software. The RNase protection assay was performed with RNA samples from two to five individual livers (for each virus). At least two independently prepared virus stocks were used for this analysis. Representative pictures are shown.

RESULTS

Immediately after injection, all Ad vectors accumulated with equal efficiencies in the liver, but only genomes of long-shafted Ads are efficiently maintained over time. To delineate the mechanisms involved in Ad accumulation in the mouse liver following intravenous application, we used a set of previously constructed Ad5-based vectors possessing modified fibers (Fig. 1) (38). Ad5/9L and Ad5/9S possess the Ad9 knob domain and long (Ad5, 22 β sheets) or short (Ad9, 7 β sheets) fiber shafts, respectively. Ad5/35L and Ad5/35S possess long (Ad5) and short (Ad35) fiber shafts and an Ad35 knob domain. Ad vectors possessing the Ad9 knob domain can infect cells in vitro via interactions with CAR (31, 38), while Ad35 fiber knob-possessing vectors can infect cells via interactions with CD46 (8). As outlined above, rodent cells in vitro do not express CD46 and are refractory to infection with Ad35 fiber knob-possessing vectors. In vivo, long-shafted Ad35 knob-possessing vectors (Ad5/35L) can infect hepatocytes as efficiently as Ad5 vectors. This infection is presumably mediated by blood factors and uptake through HSPGs and low-density lipoprotein receptor-related protein (39). Previous data suggested that this pathway cannot be used efficiently by short-shafted vectors, since the accumulation of Ad genomes and transgene expression in hepatocytes for short-shafted Ad5/35S was 1/10 that of Ad5 vectors when measured 72 h after tail vein injection (4, 36).

To analyze whether the reduced efficiency of transgene expression seen for the short-shafted non-CAR-interacting Ad5/35S vector would also be observed for the short-shafted CAR-interacting Ad5/9S variant, we administered 10^{11} particles of each Ad into the tail vein of C57BL/6 mice. Three days later, mice were sacrificed, livers were fixed in formalin, and serial sections were prepared. The analysis of GFP expression revealed that only long-shafted Ads were able to efficiently transduce hepatocytes and express the transgene by this time, regardless of the type of fiber knob domain (Fig. 2A).

To analyze the kinetics of Ad accumulation in the liver at earlier time points, we administered 10^{11} particles of each viral vector into the tail vein of C57BL/6 mice. At 30 min, 6 h, and 24 h postinfusion (p.i.), blood was flushed from the liver by cardiac saline perfusion, livers were harvested, and hepatic DNA was subjected to quantitative Southern blot analysis with a probe specific to viral DNA (Fig. 2B). At 30 min p.i., the amounts of Ad DNA in the liver were comparable for all vectors. However, at 6 h p.i., and more so at 24 h p.i., there was less viral DNA of short-shafted vectors in the liver than of the corresponding long-shafted variants. In agreement with earlier findings (52), the total amount of long-shafted Ad DNA in the liver declined by more than 80% within 24 h p.i. (Fig. 2B; compare the intensity of the viral bands to that of the standard at 30 min and 24 h). In conclusion, immediately after injection, regardless of the shaft length, viral particles are deposited equally efficiently in the liver. However, only long-shafted Ad genomes are efficiently retained in the liver over time.

At 30 min p.i., short- and long-shafted Ad5/9 and Ad5/35 particles are localized to the liver sinusoids. To analyze in more detail the localization of Ad particles within the liver at 30 min p.i., we performed electon microscopy on ultrathin liver sections. Virus particles of both long-shafted and short-shafted vectors could be found in the sinusoids and the space of Disse (Fig. 3), suggesting that all Ads are physically capable of reaching the hepatocyte surface.

Ad9 knob-possessing vectors can infect hepatocytes through CAR, but internalization for Ad5/9S is slower than that for Ad5/9L. To further corroborate the electron microscopy findings, we analyzed whether Ad particles were inside or outside liver cells within the first 30 min p.i. In these experiments, we focused on the binding to and uptake by hepatocytes of Ad particles. At 30 min after virus administration into the tail vein, the liver was perfused for 15 min with a trypsin-DNase solution to disrupt virus-receptor complexes and degrade noninternalized viral DNA. Hepatocytes were isolated by collagenase di-

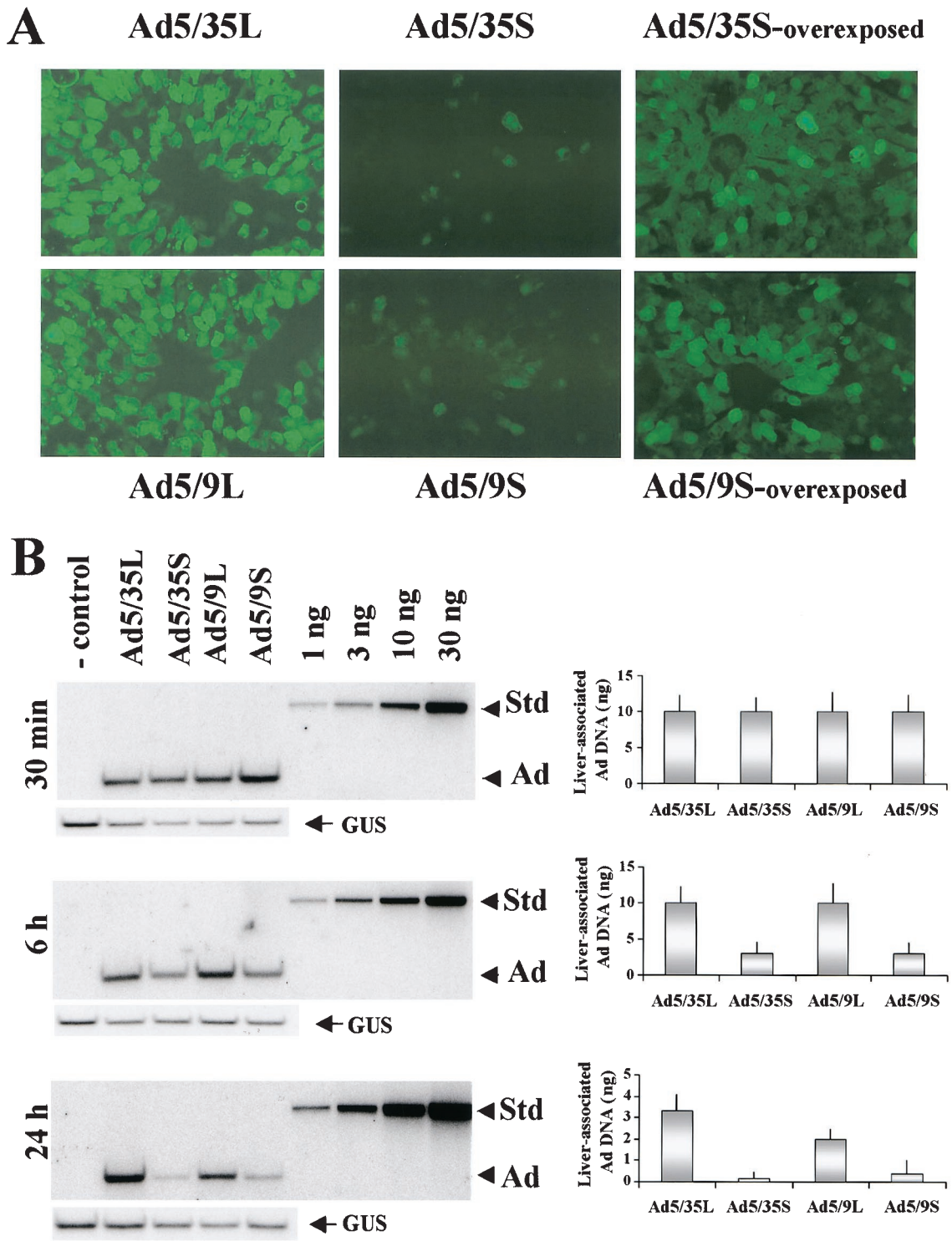

FIG. 2. In vivo transduction of hepatocytes with capsid-modified Ads and Southern blot analysis of Ad DNAs in the liver at different times after systemic vector application. (A) At 72 h after intravenous Ad injection, livers were recovered and serial sections of formalin-fixed tissues were prepared. To visualize GFP fluorescence, images of sections were taken under UV light. Representative fields are shown. Magnification, ×200. (B) At the indicated times after intravenous Ad injection, livers were recovered from mice and total DNA was purified as described in Materials and Methods. Ten micrograms of total DNA digested with HindIII enzyme was loaded on agarose gels along with serial threefold dilutions of standard (Ad5 genomic) DNA of a known concentration (Std). After transfer to Hybond N+ membranes, filters were hybridized with a mouse β-glucuronidase-specific probe to confirm equivalent loads (GUS). Subsequently, the membranes were stripped and rehybridized with an Ad-specific probe (Ad). The right panels show the quantification of vector genomes by PhosphorImager analysis ($n = 3$); error bars indicate standard deviations. Note that the absolute amount of Ad DNA significantly decreased over time (compare the intensity of the Ad bands to the intensity of the standard bands). The control was DNA purified from the livers of mice injected with PBS only.

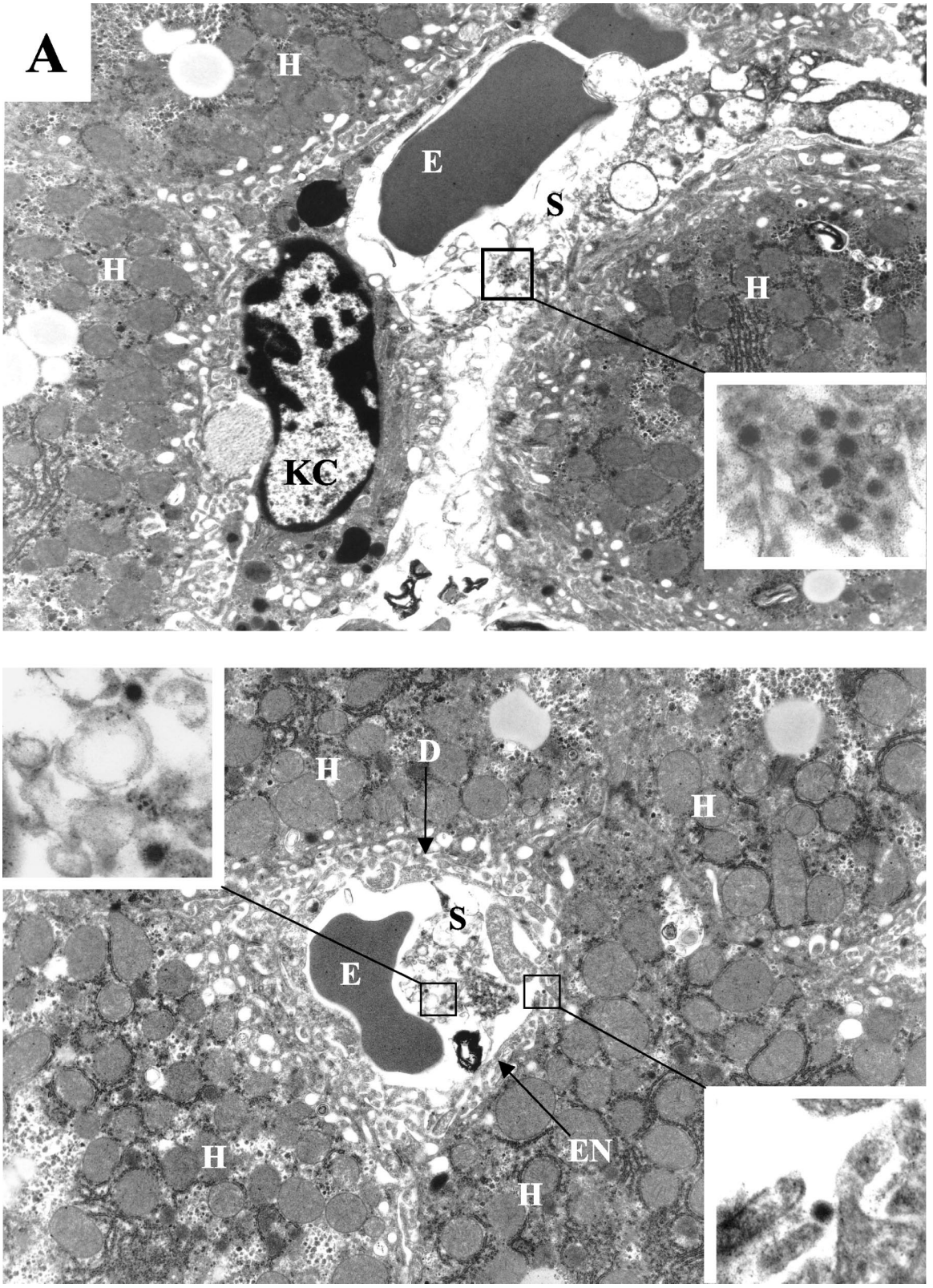

FIG. 3. Visualization of Ad distribution in liver tissue 30 min after intravenous application. (A) Ads present in hepatic sinusoids. (Upper panel) Ad5/9L. (Lower panel) Ad5/9S. (B and C) Ad particles present in the space of Disse (B) and in hepatic endosomes (C) in liver sections from Ad5/9L-injected mice. Note that Ad5/9S particles were present both in sinusoids and in the space of Disse (A, lower panel, upper and lower insets, respectively). H, hepatocyte; KC, Kupffer cell; S, sinusoid; E, erythrocyte; D, space of Disse; EN, sinusoid endothelial cell; ES, endosome. The characteristic morphology of Ad particles can be seen clearly on the enlarged images of selected areas. Magnifications: ×4,400 for main images and ×21,000 for enlarged images.

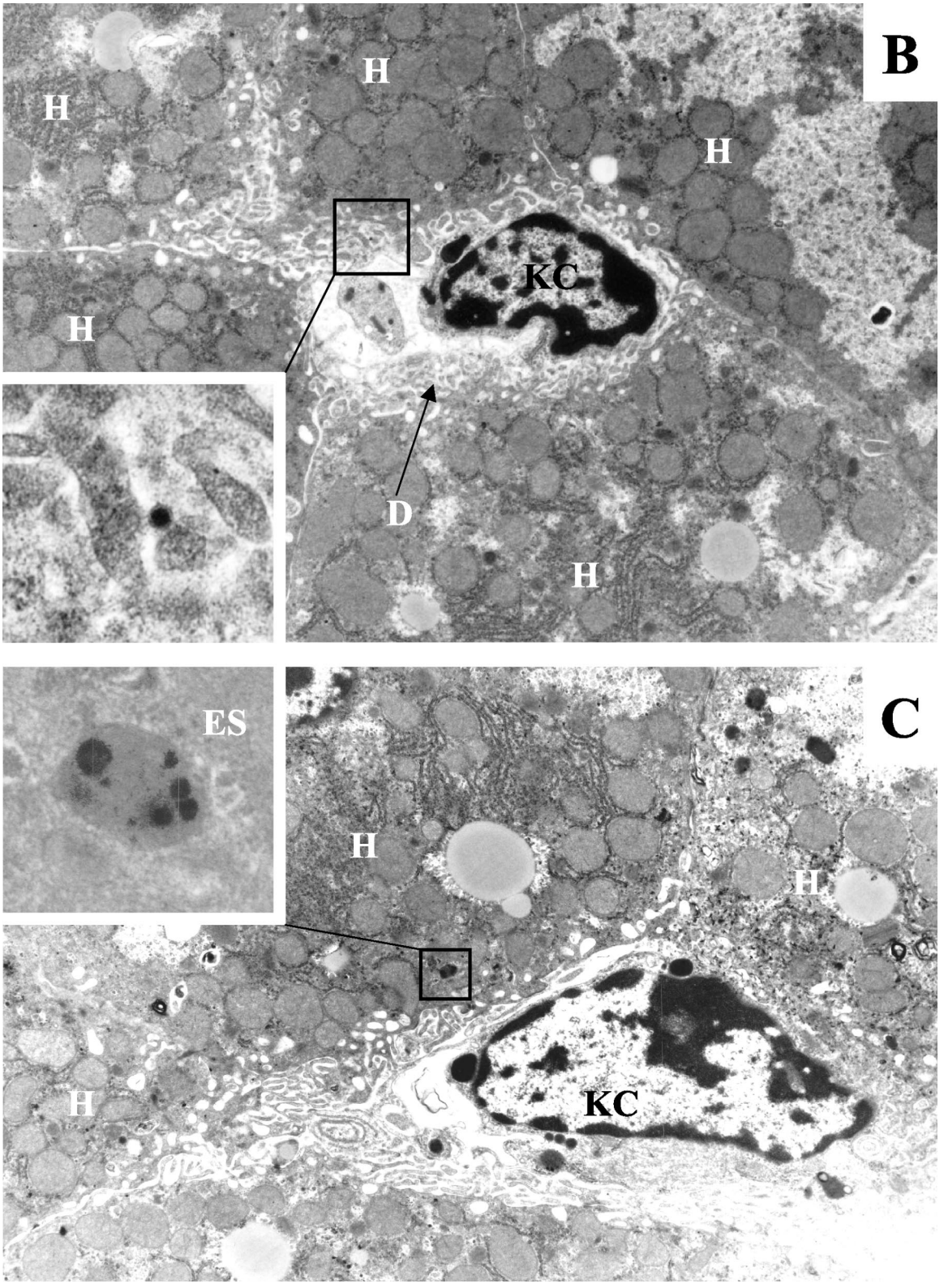

FIG. 3—*Continued*.

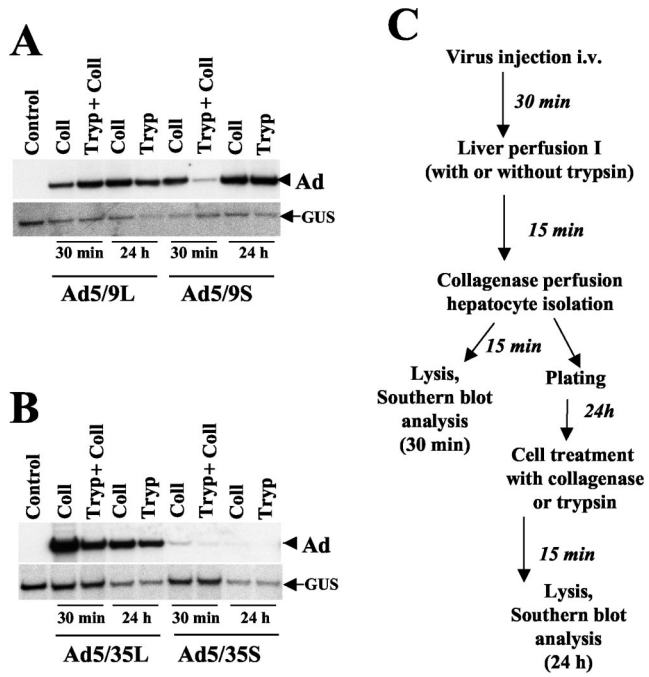

FIG. 4. Southern blot analysis of Ad DNA associated with purified liver cells at different times. (A and B) At 30 min after intravenous injection of Ad9 (A) or Ad35 (B) knob-possessing vectors, livers were perfused either with collagenase (Coll) or with trypsin (Tryp) followed by collagenase solutions. Hepatocytes were harvested as a single-cell suspension, and total DNA was purified (30-min time points). To analyze the amount of Ad DNA associated with hepatocytes at 24 h after hepatocyte purification by collagenase perfusion, plated cells were treated with collagenase-DNase or trypsin-DNase solutions prior to cell lysis and DNA purification. Purified cellular DNA was digested with HindIII and applied to agarose gels for subsequent Southern blot analysis as described in the legend to Fig. 2B. The control was DNA purified from hepatocytes harvested from the livers of mice injected with PBS only. (C) Schematic representation of experimental procedures. To analyze virus degradation in purified hepatocytes at 24 h after cell isolation, hepatocytes were purified from livers by collagenase perfusion only (liver perfusion I step was omitted). i.v., intravenously.

gestion of liver samples (Fig. 4C; also see Materials and Methods). Total DNA isolated from purified hepatocytes was analyzed by quantitative Southern blotting. In hepatocytes obtained by collagenase perfusion (without prior trypsin digestion), the amounts of the Ad5/9L and Ad5/9S vectors were comparable (Fig. 4A, 30 min). This finding was unexpected, considering that the infection of cultured cells in vitro was inefficient with short-shafted Ad5/9S due to electrostatic repulsion between the negatively charged particle and the cell surface (38). We speculate that collagenase perfusion of the liver removes some negative charge from the surface of hepatocytes, facilitating infection with Ad5/9S through CAR. When the liver was perfused with trypsin before hepatocyte isolation, the amount of the short-shafted Ad5/9S vector associated with liver cells was significantly smaller than that of the long-shafted Ad5/9L vector. This finding suggests that trypsin, but not collagenase, treatment disrupted Ad5/9S-CAR complexes (and/or digested viral particles). Furthermore, the data indicate that although the initial attachment of both Ad9 knob-possessing vectors occurred with similar efficiencies, Ad5/9S required more time for internalization into cells.

To analyze whether the fates of Ad particles with different fiber shaft lengths internalized within infected hepatocytes differ, at 30 min after Ad infusion, hepatocytes were isolated by collagenase perfusion, plated on six-well plates, and cultured for 24 h. One set of cells was treated with acollagenase-DNase solution and another set was treated with a trypsin-DNase solution to remove all extracellular virus. Southern blot analysis of hepatocellular DNA showed similar amounts of Ad5/9L and Ad5/9S vector DNAs (Fig. 4A, 24-h time point), indicating that differential intracellular degradation or retrograde transport (37) to the cell surface of Ad5/9S particles, compared to Ad5/9L particles, is not the primary mechanism for the removal of short-shafted vectors from liver cells by 24 h p.i. in our experimental settings. The presence of the same amounts of Ad5/9L and Ad5/9S genomes in hepatocytes (Fig. 4A, 24-h time point) is in conflict with the transgene expression data shown in Fig. 2A. We speculated above that collagenase perfusion of livers (performed to obtain hepatocytes) allows for the binding of Ad5/9S to CAR and for subsequent uptake by hepatocytes. On the other hand, the transgene expression data were obtained at day 3 p.i. without collagenase treatment, a situation that might make CAR accessible to Ad5/9S binding.

Ad5/35S is unable to interact with hepatocellular receptors and is therefore not taken up by hepatocytes. A similar analysis was performed with Ad35 knob-possessing vectors (Fig. 4B). First, the presence of viral DNA was analyzed immediately after collagenase perfusion. As was seen with the Ad5/9L vector, collagenase perfusion did not affect the amount of the Ad5/35L vector, indicating that collagenase treatment did not interfere with Ad35 fiber knob binding to hepatocellular receptors. However, in contrast to the results obtained for Ad5/9, collagenase perfusion reduced the amount of short-shafted Ad5/35S associated with purified hepatocytes by more than 30-fold. This finding is not unexpected because, compared to Ad5/9S, Ad5/35S cannot interact with CAR and can be washed out from the liver. Preperfusion of the liver with a trypsin-DNase solution prior to hepatocyte purification further reduced the amount of Ad5/35S vector DNA associated with purified hepatocytes. Since only a minimal amount of Ad5/35S vector genomes was associated with liver cells at 30 min p.i., the amount of Ad5/35S vector genomes associated with purified hepatocytes at 24 h p.i. was barely detectable. Taken together, these data demonstrate that although the amount of Ad5/35S genomes in the liver tissue was similar to that of Ad5/35L genomes (Fig. 2B, 30 min), the short-shafted virus was unable to efficiently interact with cellular receptors for attachment and internalization and therefore was not associated with purified cells.

To further confirm that Ad particles can be internalized during the first 30 min p.i., we purified hepatocytes 15 and 30 min after Ad infusion. These cells were plated on six-well plates, and reporter gene expression (GFP expression for Ad5/9 vectors and β-galactosidase expression for Ad5/35 vectors) was analyzed 48 h later. For Ad5/9S and Ad5/9L, efficient hepatocyte transduction occurred within 15 min p.i. (Fig. 5A). For Ad5/35L, 60% of cells purified at 15 min p.i. and more than 90% of cells purified at 30 min p.i. were positive for transgene expression (Fig. 5B). In contrast, only a few hepa-

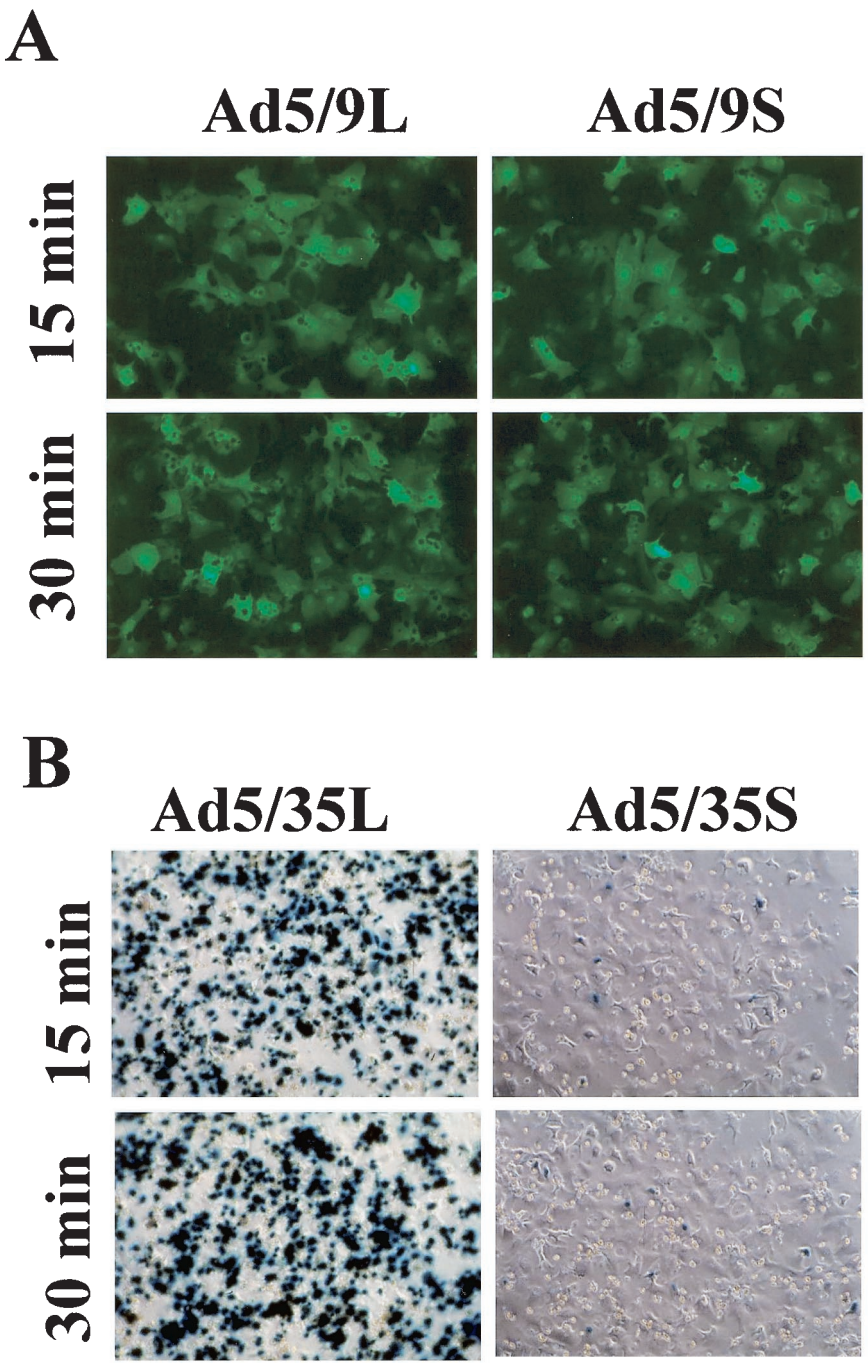

FIG. 5. Expression of reporter genes for GFP (for Ad9 knob-possessing vectors) (A) or β-galactosidase (for Ad35 knob-possessing vectors) (B) in hepatocytes purified 15 and 30 min after intravenous virus application. Hepatocytes purified by collagenase perfusion were used to seed six-well plates, and reporter gene expression was assessed 48 h later as described in Materials and Methods.

tocytes demonstrated transgene expression when Ad5/35S was infused into mice, corroborating the Southern blot data that the genomes of short-shafted Ad5/35S, although present in the liver tissue at an amount similar to that of their long-shafted counterparts, are unable to attach to and productively infect liver cells. Taken together, these results indicate that the accumulation of Ad in liver tissue shortly after intravenous administration does not depend on the interaction of viruses with liver cell receptors.

Ad5/35L is efficiently taken up by Kupffer cells via a CAR-independent, knob-dependent pathway. To investigate in more detail the distribution of Ad vectors in the liver tissue shortly after intravenous application, we labeled Ad particles with the fluorophore Cy-3 (17). At 30 min after infusion of Cy-3-labeled

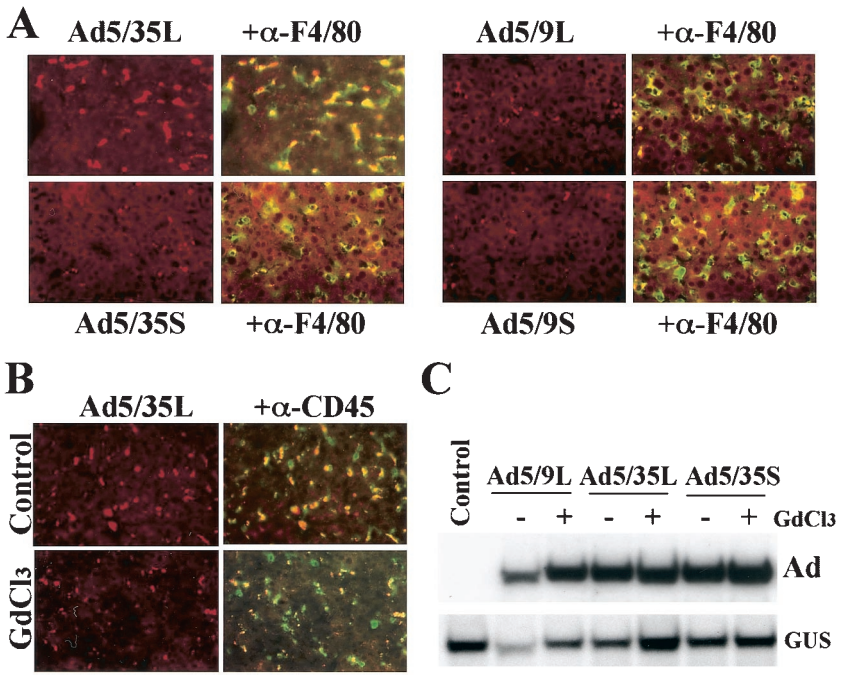

FIG. 6. Association of Ad vectors with Kupffer cells (A and B) and liver cell transduction in Kupffer cell-depleted mice (C). (A) Cy-3-labeled Ads were injected into the tail vein of C57BL/6 mice. At 30 min later, livers were recovered and immediately frozen in OCT compound. To visualize Kupffer cells, fixed liver sections were stained with anti-F4/80 antibody (green). Cy-3-labeled virus appears red. Images of representative fields were taken with red and green filters and then were superimposed to reveal the association of Ad vectors with Kupffer cells (yellow). (B) Mice were treated with gadolinium chloride ($GdCl_3$) to functionally inactivate Kupffer cells, which were stained with anti-CD45 antibody (green). At 30 min after injection of Cy-3-labeled Ads, livers were recovered, and the association of Ad vectors with Kupffer cells was evaluated. Note that in $GdCl_3$-treated mice, the association of Ad vectors with Kupffer cells was dramatically reduced. (C) Southern blot analysis of Ad genomes present in the livers of mice treated with $GdCl_3$ and normal mice ($-GdCl_3$) 30 min after systemic vector application. GUS, mouse β-glucuronidase gene. The control was liver DNA from a mouse injected with virus dilution buffer (PBS) only.

Ads, blood was flushed from the livers, and the livers were harvested and cryosectioned. While the long-shafted Ad5/35L vector formed large virus aggregates, the signals from the short-shafted Ad5/9S and Ad5/35S vectors and the long-shafted Ad5/9L vector were smaller, dim, and evenly dispersed throughout the sections (Fig. 6A). Analysis of liver sections with anti-F4/80 antibodies, which specifically stained macrophages and Kupffer cells (20), revealed that the areas of Ad5/35L accumulation overlapped the areas of positive anti-F4/80 staining, demonstrating that a significant amount of the long-shafted Ad5/35L vector is trapped by Kupffer cells at this time. Although the colocalization of Ad and F4/80 signals was also seen for the other Ads, Kupffer cell uptake of these vectors was significantly less efficient than that of Ad5/35L. Because the long-shafted Ad5/35L and Ad5/9L vectors differ only in their fiber knob domain, our data demonstrate that the Ad fiber knob is the primary determinant within the Ad capsid responsible for Ad accumulation in Kupffer cells. Furthermore, because Ad5/35L does not interact with CAR, Kupffer cell uptake by this vector is CAR independent.

Independently of the fiber length or the nature of the knob domain, Kupffer cells are not the major reservoir in the liver for systemically applied Ad. To understand the role of Kupffer cells in the fate of Ad5/35L, Kupffer cells were functionally inactivated by gadolinium chloride ($GdCl_3$) administration into mice, and the levels of Ad accumulation in the livers of normal mice and $GdCl_3$-treated mice were compared. The administration of $GdCl_3$ 30 min and 6 h prior to virus injection dramatically reduced the ability of Kupffer cells to accumulate long-shafted Cy-3-labeled Ad5/35L (Fig. 6B). Nonetheless, quantitative Southern blot analysis of Ad genomes accumulated in the liver tissue at 30 min p.i. demonstrated similar levels of Ad DNA in both normal and $GdCl_3$-treated mice for the long-shafted Ad5/9L and Ad5/35L vectors (Fig. 6C) and the short-shafted Ad5/35S (Fig. 6C) and Ad5/9S (data not shown) vectors.

In conclusion, from the finding that the accumulation of both long-shafted and short-shafted vectors in the liver occurred at similar levels (Fig. 3 and 4), one can conclude that Kupffer cells are not the major reservoir for intravenously injected Ad in liver tissue.

Short-shafted Ads induce less cytokine gene expression in liver cells after systemic application. The intravenous administration of Ad results in the initiation of strong innate immune responses in animals and humans (29). To evaluate whether efficient liver cell infection is required for the initiation of innate and inflammatory responses, we analyzed levels of hepatic cytokine and chemokine gene transcription as well as levels of proinflammatory cytokines and ALT in serum after intravenous Ad administration. These analyses revealed that the mRNA levels for most of the genes analyzed at 30 min after virus administration were significantly lower for short-

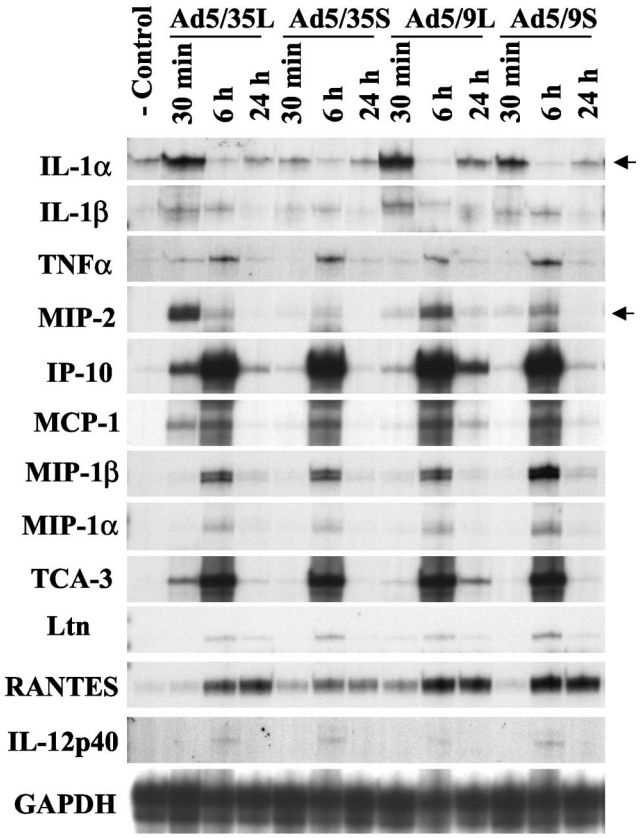

FIG. 7. Short-shafted vectors induce lower levels of proinflammatory cytokine and chemokine gene transcription after systemic Ad administration. At the indicated times, total liver RNA was purified, and the mRNA levels for proinflammatory genes were analyzed by an RNase protection assay as described in Materials and Methods. Upregulated IL-1α and MIP-2 gene mRNA levels are indicated by arrows. IP-10, interferon gamma-inducible protein-10; MCP-1, monocyte chemoattractant protein; TCA-3, T-cell activation gene-3; GAPDH, glyceraldehyde 3-phosphate dehydrogenase.

shafted vectors than for their long-shafted counterparts (Fig. 7, 30 min). Among all analyzed genes, the transcription levels for the IL-1α, IL-1β, and MIP-2 genes were highest shortly after long-shafted Ad5/35L vector administration. Notably, Ad5/35L was more efficiently taken up by Kupffer cells than the other Ads (Fig. 6A). In particular, the levels of IL-1α increased by 20-fold and the levels of MIP-2 increased by more than 25-fold for Ad5/35L compared to preinjection levels. Although the upregulation of IL-1α gene transcription in the liver after the administration of the Ad5/9L vector was similar to that seen with the Ad5/35L vector, the levels of MIP-2 mRNA were significantly lower with Ad5/9L vector application than with Ad5/35L vector application. Nonetheless, the majority of the genes analyzed were strongly upregulated after injection of the long-shafted Ad5/9L vector, compared to its short-shafted counterpart. Clearly, the delineation of pathways activated upon Ad uptake requires further investigation.

Importantly for Ad5/35S, the mRNA levels for IL-1α were only slightly elevated and those for MIP-2 were nearly unchanged compared to preinjection levels. Notably, MIP-2 was suggested to be the primary chemokine responsible for the attraction of neutrophils to the liver, an event which subsequently causes liver damage (20). The low levels of MIP-2 chemokine gene expression after the administration of the Ad5/35S and Ad5/9L vectors demonstrate that efficient infection of Kupffer cells most likely is required for its upregulation.

Significant upregulation of interferon gamma-inducible protein-10 (IP-10) and T-cell activation gene-3 (TCA-3) chemokine mRNA levels (more than 300-fold above the baseline) at 6 h p.i. did not depend on the length of the Ad fiber shaft domain or the nature of the fiber knob domain. The delayed upregulation (6 or 24 h) of these genes in the liver may have more complex mechanisms, potentially involving factors secreted from the spleen, peripheral blood mononuclear cells, and/or cells in the lymph node upon Ad infection, and apparently does not require efficient liver cell transduction.

Levels in serum of TNF-α, IL-6, and ALT are higher for long-shafted Ads. Analysis of serum cytokine levels revealed that for all analyzed proteins, peak levels were seen at 6 h p.i. (Fig. 8). Importantly, the levels of TNF-α and IL-6 were significantly higher for long-shafted vectors than for their short-shafted counterparts. The levels of IFN-γ and monocyte chemoattractant protein 1 were higher for the Ad5/9L vector than for its short-shafted counterpart and were not significantly different between long- and short-shafted Ad35 knob-possessing vectors.

The assessment of the overall hepatotoxicity at 24 h after intravenous virus administration by measurement of serum ALT levels revealed that the highest degree of hepatic injury was observed after injection of long-shafted Ads. The serum ALT levels observed after administration of short-shafted vectors were only slightly elevated above preinjection levels, demonstrating that viruses which are inefficient at infecting liver cells (and potentially cells in other organs) are also unable to induce hepatocellular damage.

DISCUSSION

In this study, we used Ad vectors with modified fibers to understand the morphological structures and mechanisms that govern the early accumulation of Ad in the liver. The Ad vectors varied in two fiber domains that have been found to determine the specificity and efficacy of Ad infection, the fiber shaft and the fiber knob (28, 31, 38, 47, 53). The fiber knob largely determines Ad tropism. Here we used the Ad9 knob, known to bind to CAR, and the Ad35 knob, which binds CD46. Efficient infection in vitro through CAR requires a long, flexible shaft (38, 42, 47, 53), whereas the efficiency of infection through CD46 seems to be independent of the fiber shaft length.

Within 30 min after tail vein injection, all vectors, independent of the nature of the fiber knob or shaft, accumulated equally efficiently in the liver sinusoids. However, the amount of viral genomes and the number of transgene-expressing hepatocytes were more than 10-fold lower for the short-shafted vectors (Ad5/9S and Ad5/35S) at 24 h p.i. than for their long-shafted counterparts. These data are consistent with a recent study of long- and short-shafted Ad5/40 vectors by Nakamura et al. (28). They also found no significant differences in the amounts of viral DNA between CAR-binding and non-CAR-binding Ad vectors in the liver, corroborating the notion that

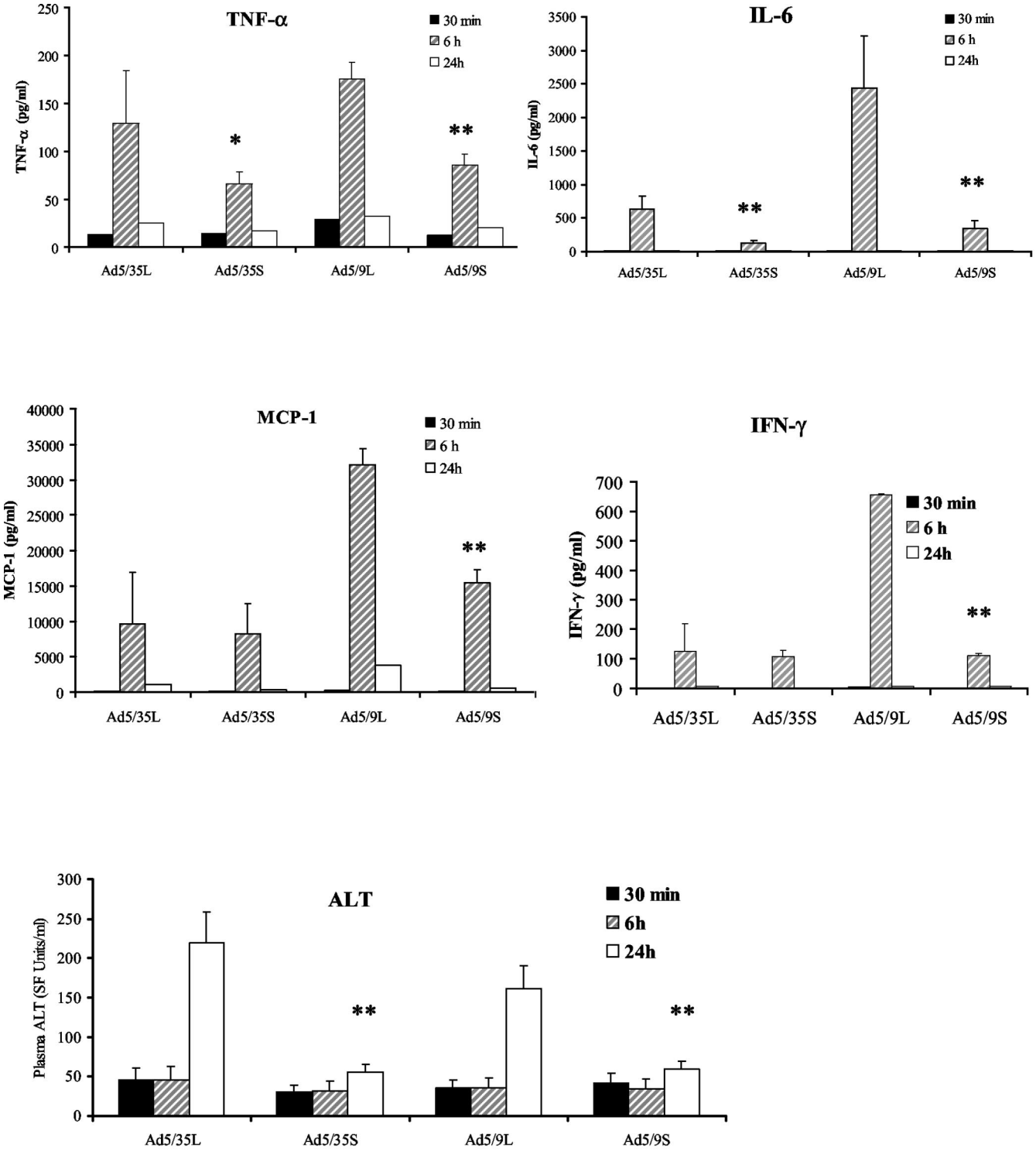

FIG. 8. Levels in plasma of proinflammatory cytokines, chemokines, and ALT are lower for short-shafted Ads than for long-shafted Ads. At the indicated times, plasma samples from three individual mice per virus treatment group were collected and analyzed in duplicate for levels of proinflammatory cytokines and ALT as described in Materials and Methods. Error bars indicate standard deviations. A single asterisk indicates a P value of <0.05; double asterisks indicate a P value of <0.01.

early Ad accumulation in the liver does not depend on an interaction with CAR.

Upon accumulation within the liver sinusoids, long-shafted Ad5/9L and Ad5/35L efficiently infect hepatocytes. Both CAR- and non-CAR-interacting vectors are equally efficient in hepatocyte transduction in vivo, indicating that the CAR pathway is not the dominant pathway for in vivo infection. The KKTK shaft motif was recently suggested to mediate liver infection

through HSPGs in vivo (42). Shayakhmetov et al. have found an additional pathway which appears to dominate both the CAR and the shaft motif pathways (39). When a liver is perfused with Ad without blood, only minimal hepatocyte transduction is seen with a KKTK shaft motif-containing, non-CAR-interacting Ad5/35L vector, whereas transduction with a CAR-interacting Ad5L vector is not significantly decreased (39). The latter finding argues against the hypotheses that CAR is not accessible in the liver in vivo and that direct KKTK shaft motif binding to HSPGs is the primary pathway of liver cell infection in vivo.

Short-shafted Ads are unable to infect liver cells through CAR, through the KKTK shaft motif, or through blood factors. Due to these features, they are not taken up by liver cells and are probably degraded within the sinusoids. Importantly, short-shafted Ads did not cause innate toxicity in mice and therefore might represent a useful scaffold for the insertion of targeting ligands. However, when using short-shafted fibers, one must consider that certain ligand-receptor interactions require long fiber shafts. For example, the CAR-knob interaction is not efficient with short fiber shafts, likely because of either steric hindrances that affect the interaction with CAR and/or integrins or repulsion between negative charges on the virion and the cell surface (28, 38, 47, 53). Theoretically, receptors for short-shafted Ads should protrude over the glycocalyx or should be internal (without the requirement of binding secondary receptors, such as integrins). A natural receptor for short-shafted group B Ads is CD46 (8). CD46 is overexpresssed on important target cells for gene therapy, including tumor cells (10, 14, 26, 45) and potential hematopoietic stem cells (7, 22), and vectors that target CD46 are becoming useful tools for gene therapy. Both chimeric Ad5 vectors with E1 deleted but possessing Ad35 fibers (9, 25, 30, 32, 36, 40, 48) and vectors completely derived from Ad35 have been developed, and the generation of helper-dependent Ad35 or other group B Ad vectors is in progress (44). As shown in this study, in addition to the useful tropism, Ad35 fiber-possessing Ad vectors avoid liver sequestration and innate toxicity. Furthermore, there is a low serum prevalence of neutralizing antibodies against Ad35 in healthy individuals in different parts of the world (48).

To further prove that Ad35 fiber-containing vectors are safer than Ad5 vectors, studies with transgenic mice that express CD46 in a pattern that mimics that in humans (13) must be conducted. Preliminary data indicate that the amount of Ad5/35 vector DNA in the liver of CD46-transgenic mice is ~10 times lower than that of Ad5 vector DNA after systemic vector application (8).

Kupffer cells account for 80 to 90% of resident macrophages in the entire body (3) and, after systemic administration, efficiently take up Ad particles. The mechanisms of Ad uptake and subsequent Kupffer cell activation are a matter of intense investigation. This study and others (20) have established that Ad uptake by Kupffer cells is CAR independent. The contribution of the KKTK shaft motif and/or blood factors remains to be shown. Furthermore, in preimmunized animals, Ad-antibody complexes may be taken up by Kupffer cells through Fc receptors. In this context, it is notable that, when high Ad doses were used in preimmunized nonhuman primates, new toxic effects that were not observed in naive animals were found (46).

As outlined earlier, at doses usually used to achieve efficient transgene expression in target cells (i.e., $>2 \times 10^9$ PFU/mouse for the transduction of hepatocytes or tumor cells in tumor models), the Kupffer cell system becomes saturated and virus disseminates and infects other cell types. Furthermore, our data and data obtained by Liu et al. (20) demonstrate that in Kupffer cell-depleted animals, the amount of viral DNA found in the liver early after injection (30 min) is not significantly decreased, indicating that although Kupffer cells efficiently take up Ad, they are not a major reservoir of Ad in the liver. It seems that the majority of virus remains in the liver sinusoids. Schiedner et al. (33) suggested recently that the activation of Kupffer cells within minutes after Ad injection results in the release of factors which, in turn, activate endothelial cells. These events are associated with thickening of the endothelium, presumably leading to a change in fenestration size. One could speculate that this effect might cause a blockage of transendothelial Ad transport, resulting in Ad particles being retained inside the sinusoids or the space of Disse. This situation would subject vector particles to increased clearance from the liver by the bloodstream and circulating innate effector cells (32). Arguing against this model is the recent finding that although short-shafted Ad5/35 vectors did not infect mouse tissue and were not taken up by Kupffer cells, they did not transduce liver metastases derived from CD46-positive human tumor cells more efficiently than nontargeted Ad5 vectors (4). This finding indicates that the mechanisms that govern transendothelial transport of Ad particles are more complex. For example, the shafts of Ad5/35S (which lacks a shaft domain that confers flexibility in Ad5) might not be flexible enough to pass through the endothelial fenestrae. Furthermore, it is possible that Ad, while inside the sinusoids, must contact its cellular receptors through the fiber and is then actively pulled through the fenestrae. Apparently, Ad transendothelial transport is facilitated by the long fiber shaft.

First-generation Ads induced a biphasic pattern of inflammatory cytokine gene expression in the liver after systemic Ad injection. A first peak is seen at about 6 h p.i. and is associated with virus uptake. A second peak appears at day 4 or 5 p.i. and is associated with viral gene expression (19). Considering the relatively low capacity of Kupffer cells to take up Ad, the question arises as to what other cytokine-producing cell types interact with Ad. Studies by Lui et al. (20) showed that RGD mutants induced less E-selectin and VCAM-1 gene expression in the liver, indicating that Ad infects endothelial cells through integrins, which lead to their activation. Furthermore, peripheral blood leukocytes that infiltrate the liver upon Ad injection may interact with Ad vectors, resulting in cytokine expression. The induction of IL-6, granulocyte-macrophage colony-stimulating factor, and a panel of chemokines upon Ad interaction with peripheral blood cells has been reported (11). Clearly, in situ hybridization or in situ reverse transcription-PCR for cytokine mRNA in liver sections will help to delineate the relative contributions of different cell types in hepatic cytokine expression.

The finding that short-shafted Ads do not cause cytokine expression and release or hepatotoxicity provides a rationale to use these vectors for targeting purposes. We have also shown

that short-shafted Ads are a useful tool for analyzing the mechanisms involved in Ad liver sequestration. Clearly, more studies are required to delineate the precise molecular mechanisms of Ad clearance from the liver.

ACKNOWLEDGMENTS

We thank Anuj Gaggar and Daniel Stone for helpful discussions.

This work was supported by grants from the NIH (R01 CA80192, P30 DK47754, and HL-00-008) and the Cystic Fibrosis Foundation.

REFERENCES

1. **Alemany, R., and D. T. Curiel.** 2001. CAR-binding ablation does not change biodistribution and toxicity of adenoviral vectors. Gene Ther. **8:**1347–1353.
2. **Alemany, R., K. Suzuki, and D. T. Curiel.** 2000. Blood clearance rates of adenovirus type 5 in mice. J. Gen. Virol. **81:**2605–2609.
3. **Arii, S., and M. Imamura.** 2000. Physiological role of sinusoidal endothelial cells and Kupffer cells and their implication in the pathogenesis of liver injury. J. Hepatobiliary Pancreat. Surg. **7:**40–48.
4. **Bernt, K., S. Ni, Z.-Y. Li, D. M. Shayakhmetov, and A. Lieber.** 2003. The effect of sequestration by nontarget tissues on anti-tumor efficacy of systemically applied, conditionally replicating adenovirus vectors. Mol. Ther. **8:**746–755.
5. **Borgland, S. L., G. P. Bowen, N. C. Wong, T. A. Libermann, and D. A. Muruve.** 2000. Adenovirus vector-induced expression of the C-X-C chemokine IP-10 is mediated through capsid-dependent activation of NF-κB. J. Virol. **74:**3941–3947.
6. **Carlson, C. A., D. S. Steinwaerder, H. Stecher, D. M. Shayakhmetov, and A. Lieber.** 2002. Rearrangements in adenoviral genomes mediated by inverted repeats. Methods Enzymol. **346:**277–292.
7. **Cho, S. W., T. J. Oglesby, B. L. Hsi, E. M. Adams, and J. P. Atkinson.** 1991. Characterization of three monoclonal antibodies to membrane co-factor protein (MCP) of the complement system and quantification of MCP by radioassay. Clin. Exp. Immunol. **83:**257–261.
8. **Gaggar, A., D. M. Shayakhmetov, and A. Lieber.** 2003. CD46 is a cellular receptor for group B adenoviruses. Nat. Med. **9:**1408–1412.
9. **Gao, W., P. D. Robbins, and A. Gambotto.** 2003. Human adenovirus type 35: nucleotide sequence and vector development. Gene Ther. **10:**1941–1949.
10. **Hara, T., A. Kojima, H. Fukuda, T. Masaoka, Y. Fukumori, M. Matsumoto, and T. Seya.** 1992. Levels of complement regulatory proteins, CD35 (CR1), CD46 (MCP) and CD55 (DAF) in human haematological malignancies. Br. J. Haematol. **82:**368–373.
11. **Higginbotham, J. N., P. Seth, R. M. Blaese, and W. J. Ramsey.** 2002. The release of inflammatory cytokines from human peripheral blood mononuclear cells in vitro following exposure to adenovirus variants and capsid. Hum. Gene Ther. **13:**129–141.
12. **Inoue, N., M. Ikawa, T. Nakanishi, M. Matsumoto, M. Nomura, T. Seya, and M. Okabe.** 2003. Disruption of mouse CD46 causes an accelerated spontaneous acrosome reaction in sperm. Mol. Cell. Biol. **23:**2614–2622.
13. **Kemper, C., M. Leung, C. B. Stephensen, C. A. Pinkert, M. K. Liszewski, R. Cattaneo, and J. P. Atkinson.** 2001. Membrane cofactor protein (MCP; CD46) expression in transgenic mice. Clin. Exp. Immunol. **124:**180–189.
14. **Kinugasa, N., T. Higashi, K. Nouso, H. Nakatsukasa, Y. Kobayashi, M. Ishizaki, N. Toshikuni, K. Yoshida, S. Uematsu, and T. Tsuji.** 1999. Expression of membrane cofactor protein (MCP, CD46) in human liver diseases. Br. J. Cancer **80:**1820–1825.
15. **Kuzmin, A. I., M. J. Finegold, and R. C. Eisensmith.** 1997. Macrophage depletion increases the safety, efficacy and persistence of adenovirus-mediated gene transfer in vivo. Gene Ther. **4:**309–316.
16. **Leissner, P., V. Legrand, Y. Schlesinger, D. A. Hadji, M. van Raaij, S. Cusack, A. Pavirani, and M. Mehtali.** 2001. Influence of adenoviral fiber mutations on viral encapsidation, infectivity and in vivo tropism. Gene Ther. **8:**49–57.
17. **Leopold, P. L., B. Ferris, I. Grinberg, S. Worgall, N. R. Hackett, and R. G. Crystal.** 1998. Fluorescent virions: dynamic tracking of the pathway of adenoviral gene transfer vectors in living cells. Hum. Gene Ther. **9:**367–378.
18. **Lieber, A., C. Y. He, L. Meuse, C. Himeda, C. Wilson, and M. A. Kay.** 1998. Inhibition of NF-κB activation in combination with bcl-2 expression allows for persistence of first-generation adenovirus vectors in the mouse liver. J. Virol. **72:**9267–9277.
19. **Lieber, A., C. Y. He, L. Meuse, D. Schowalter, I. Kirillova, B. Winther, and M. A. Kay.** 1997. The role of Kupffer cell activation and viral gene expression in early liver toxicity after infusion of recombinant adenovirus vectors. J. Virol. **71:**8798–8807.
20. **Liu, Q., A. K. Zaiss, P. Colarusso, K. Patel, G. Haljan, T. J. Wickham, and D. A. Muruve.** 2003. The role of capsid-endothelial interactions in the innate immune response to adenovirus vectors. Hum. Gene Ther. **14:**627–643.
21. **Lozier, J. N., G. Csako, T. H. Mondoro, D. M. Krizek, M. E. Metzger, R. Costello, J. G. Vostal, M. E. Rick, R. E. Donahue, and R. A. Morgan.** 2002. Toxicity of a first-generation adenoviral vector in rhesus macaques. Hum. Gene Ther. **13:**113–124.
22. **Manchester, M., K. A. Smith, D. S. Eto, H. B. Perkin, and B. E. Torbett.** 2002. Targeting and hematopoietic suppression of human $CD34^+$ cells by measles virus. J. Virol. **76:**6636–6642.
23. **Martin, K., A. Brie, P. Saulnier, M. Perricaudet, P. Yeh, and E. Vigne.** 2003. Simultaneous CAR- and α_V integrin-binding ablation fails to reduce Ad5 liver tropism. Mol. Ther. **8:**485–494.
24. **Mittereder, N., K. L. March, and B. C. Trapnell.** 1996. Evaluation of the concentration and bioactivity of adenovirus vectors for gene therapy. J. Virol. **70:**7498–7509.
25. **Mizuguchi, H., and T. Hayakawa.** 2002. Adenovirus vectors containing chimeric type 5 and type 35 fiber proteins exhibit altered and expanded tropism and increase the size limit of foreign genes. Gene **285:**69–77.
26. **Murray, K. P., S. Mathure, R. Kaul, S. Khan, L. F. Carson, L. B. Twiggs, M. G. Martens, and A. Kaul.** 2000. Expression of complement regulatory proteins—CD 35, CD 46, CD 55, and CD 59—in benign and malignant endometrial tissue. Gynecol. Oncol. **76:**176–182.
27. **Muruve, D. A., M. J. Barnes, I. E. Stillman, and T. A. Libermann.** 1999. Adenoviral gene therapy leads to rapid induction of multiple chemokines and acute neutrophil-dependent hepatic injury in vivo. Hum. Gene Ther. **10:**965–976.
28. **Nakamura, T., K. Sato, and H. Hamada.** 2003. Reduction of natural adenovirus tropism to the liver by both ablation of fiber-coxsackievirus and adenovirus receptor interaction and use of replaceable short fiber. J. Virol. **77:**2512–2521.
29. **Raper, S. E., N. Chirmule, F. S. Lee, N. A. Wivel, A. Bagg, G. Gao, J. M. Wilson, and M. L. Batshaw.** 2003. Fatal systemic inflammatory response syndrome in a ornithine transcarbamylase deficient patient following adenoviral gene transfer. Mol. Genet. Metab. **80:**148–158.
30. **Reddy, P. S., S. Ganesh, M. P. Limbach, T. Brann, A. Pinkstaff, M. Kaloss, M. Kaleko, and S. Connelly.** 2003. Development of adenovirus serotype 35 as a gene transfer vector. Virology **311:**384–393.
31. **Roelvink, P. W., A. Lizonova, J. G. Lee, Y. Li, J. M. Bergelson, R. W. Finberg, D. E. Brough, I. Kovesdi, and T. J. Wickham.** 1998. The coxsackievirus-adenovirus receptor protein can function as a cellular attachment protein for adenovirus serotypes from subgroups A, C, D, E, and F. J. Virol. **72:**7909–7915.
32. **Sakurai, F., H. Mizuguchi, T. Yamaguchi, and T. Hayakawa.** 2003. Characterization of in vitro and in vivo gene transfer properties of adenovirus serotype 35 vector. Mol. Ther. **8:**813–821.
33. **Schiedner, G., W. Bloch, S. Hertel, M. Johnston, V. Dries, G. Vraga, N. van Rooijen, and S. Kochanek.** 2003. A hemodynamic response to intravenous adenovirus vector particles is caused by systemic Kupffer cell-mediated activation of endothelial cells. Hum. Gene Ther. **14:**1631–1641.
34. **Schiedner, G., S. Hertel, M. Johnston, V. Dries, N. van Rooijen, and S. Kochanek.** 2003. Selective depletion or blockade of Kupffer cells leads to enhanced and prolonged hepatic transgene expression using high-capacity adenoviral vectors. Mol. Ther. **7:**35–43.
35. **Segerman, A., J. P. Atkinson, M. Marttila, V. Dennerquist, G. Wadell, and N. Arnberg.** 2003. Adenovirus type 11 uses CD46 as a cellular receptor. J. Virol. **77:**9183–9191.
36. **Shayakhmetov, D. M., Z. Y. Li, S. Ni, and A. Lieber.** 2002. Targeting of adenovirus vectors to tumor cells does not enable efficient transduction of breast cancer metastases. Cancer Res. **62:**1063–1068.
37. **Shayakhmetov, D. M., Z. Y. Li, V. Ternovoi, A. Gaggar, H. Gharwan, and A. Lieber.** 2003. The interaction between the fiber knob domain and the cellular attachment receptor determines the intracellular trafficking route of adenoviruses. J. Virol. **77:**3712–3723.
38. **Shayakhmetov, D. M., and A. Lieber.** 2000. Dependence of adenovirus infectivity on length of the fiber shaft domain. J. Virol. **74:**10274–10286.
39. **Shayakhmetov, D. M., S. Ni, A. Gaggar, V. Krasnykh, and A. Lieber.** 2003. Binding of adenovirus knob to blood coagulation factors mediates CAR-independent liver tropism. Mol. Ther. **7:**S165.
40. **Shayakhmetov, D. M., T. Papayannopoulou, G. Stamatoyannopoulos, and A. Lieber.** 2000. Efficient gene transfer into human $CD34^+$ cells by a retargeted adenovirus vector. J. Virol. **74:**2567–2583.
41. **Smith, T., N. Idamakanti, H. Kylefjord, M. Rollence, L. King, M. Kaloss, M. Kaleko, and S. C. Stevenson.** 2002. In vivo hepatic adenoviral gene delivery occurs independently of the coxsackievirus-adenovirus receptor. Mol. Ther. **5:**770–779.
42. **Smith, T. A., N. Idamakanti, M. L. Rollence, J. Marshall-Neff, J. Kim, K. Mulgrew, G. R. Nemerow, M. Kaleko, and S. C. Stevenson.** 2003. Adenovirus serotype 5 fiber shaft influences in vivo gene transfer in mice. Hum. Gene Ther. **14:**777–787.
43. **Stein, C. S., J. L. Pemberton, N. van Rooijen, and B. L. Davidson.** 1998. Effects of macrophage depletion and anti-CD40 ligand on transgene expression and redosing with recombinant adenovirus. Gene Ther. **5:**431–439.
44. **Stone, D., H.-J. Wang, A. Furthmann, V. Sandig, and A. Lieber.** 2003. A helper-dependent adenovirus vector system based on group B serotype 11. Mol. Ther. **7:**S192.
45. **Thorsteinsson, L., G. M. O'Dowd, P. M. Harrington, and P. M. Johnson.** 1998. The complement regulatory proteins CD46 and CD59, but not CD55,

are highly expressed by glandular epithelium of human breast and colorectal tumour tissues. APMIS **106:**869–878.

46. **Varnavski, A. N., Y. Zhang, M. Schnell, J. Tazelaar, J. P. Louboutin, Q. C. Yu, A. Bagg, G. P. Gao, and J. M. Wilson.** 2002. Preexisting immunity to adenovirus in rhesus monkeys fails to prevent vector-induced toxicity. J. Virol. **76:**5711–5719.
47. **Vigne, E., J. F. Dedieu, A. Brie, A. Gillardeaux, D. Briot, K. Benihoud, M. Latta-Mahieu, P. Saulnier, M. Perricaudet, and P. Yeh.** 2003. Genetic manipulations of adenovirus type 5 fiber resulting in liver tropism attenuation. Gene Ther. **10:**153–162.
48. **Vogels, R., D. Zuijdgeest, R. van Rijnsoever, E. Hartkoorn, I. Damen, M. P. de Bethune, S. Kostense, G. Penders, N. Helmus, W. Koudstaal, M. Cecchini, A. Wetterwald, M. Sprangers, A. Lemckert, O. Ophorst, B. Koel, M. van Meerendonk, P. Quax, L. Panitti, J. Grimbergen, A. Bout, J. Goudsmit, and M. Havenga.** 2003. Replication-deficient human adenovirus type 35 vectors for gene transfer and vaccination: efficient human cell infection and bypass of preexisting adenovirus immunity. J. Virol. **77:**8263–8271.
49. **Vrancken Peeters, M. J., A. L. Perkins, and M. A. Kay.** 1996. Method for multiple portal vein infusions in mice: quantitation of adenovirus-mediated hepatic gene transfer. BioTechniques **20:**278–285.
50. **Wickham, T. J., P. Mathias, D. A. Cheresh, and G. R. Nemerow.** 1993. Integrins alpha v beta 3 and alpha v beta 5 promote adenovirus internalization but not virus attachment. Cell **73:**309–319.
51. **Wolff, G., S. Worgall, N. van Rooijen, W. R. Song, B. G. Harvey, and R. G. Crystal.** 1997. Enhancement of in vivo adenovirus-mediated gene transfer and expression by prior depletion of tissue macrophages in the target organ. J. Virol. **71:**624–629.
52. **Worgall, S., G. Wolff, E. Falck-Pedersen, and R. G. Crystal.** 1997. Innate immune mechanisms dominate elimination of adenoviral vectors following in vivo administration. Hum. Gene Ther. **8:**37–44.
53. **Wu, E., L. Pache, D. J. Von Seggern, T. M. Mullen, Y. Mikyas, P. L. Stewart, and G. R. Nemerow.** 2003. Flexibility of the adenovirus fiber is required for efficient receptor interaction. J. Virol. **77:**7225–7235.